Environmental Science
Water Research & Technology

ROYAL SOCIETY OF CHEMISTRY

PAPER

View Article Online
View Journal | View Issue

Cite this: *Environ. Sci.: Water Res. Technol.*, 2020, **6**, 2454

Response surface methodology directed adsorption of chlorate and chlorite onto MIEX resin and study of chemical properties†

Yiqiong Yang, Zenghui Zheng, Dongfeng Zhang and Xiaodong Zhang *

Received 9th November 2019,
Accepted 2nd January 2020

DOI: 10.1039/c9ew01003c

rsc.li/es-water

This study investigates the adsorption behaviors of chlorate and chlorite by MIEX resin, and determines the optimal conditions for the removal rate by utilizing response surface methodology. The chemical properties of the solution, such as pH, coexistent anions and ion strength, have great influences on the adsorption of chlorate and chlorite. The adsorption capacities of chlorate and chlorite by MIEX are 525 and 398 mg L^{-1}, respectively. When the pH is close to neutral, the removal rate of chlorate and chlorite on MIEX is the best. Sulfate radicals have a damaging influence on the adsorption of chlorate and chlorite on MIEX, leading to a low adsorption capacity. The initial adsorption kinetics of chlorate and chlorite adsorption on MIEX follows the intra-particle diffusion-controlled adsorption. The Box–Behnken design method is successfully used to establish a quadratic polynomial mode for predicting the removal efficiency of chlorate and chlorite, which is composed of three variables (adsorbent dosage, reaction time and initial concentration). The optimal removal conditions are: dosage 6.67 mL L^{-1}, reaction time 45.26 min, initial concentration 3.08 mg L^{-1} for chlorate; and dosage 9.62 mL L^{-1}, reaction time 46.36 min, initial concentration 3.04 mg L^{-1} for chlorite. According to the results, the adsorbent dosage has a strong interaction with the chlorate or chlorite concentration and reaction time, which has a significant impact on the optimization of the chlorate and chlorite removal process using MIEX. According to FTIR spectra, the adsorption mechanism for chlorate and chlorite is anion exchange.

Water impact

The DBP of chlorine dioxide, chlorate and chlorite can cause subchronic and acute exposure to hematological reactions, leading to oxidative damage of erythrocytes, which results in methemoglobin and hemolytic anemia. Therefore, mitigating chlorate and chlorite pollution is imminent. This study investigated the adsorption behaviors of chlorate and chlorite by MIEX resin, and the conditions required to achieve an optimal removal rate using response surface methodology.

1. Introduction

Maintaining a healthy environment is very important for human survival. Recently, environmental pollution has attracted the increasing attention of researchers.[1–5] Among its various forms, drinking water pollution greatly threatens human survival. Therefore, ensuring the safety of water is one of the greatest public safety problems.[6] The process of providing safe water to the public requires the addition of chemical disinfectants, which is a key step in reducing the incidence of water-borne diseases and inhibiting biofilm formation.[7] However, common disinfectants may produce disinfection by-products (DBPs), which may pose a threat to human health. As the DBPs of chlorine dioxide, chlorate and chlorite can cause subchronic and acute exposure to hematological reactions, leading to oxidative damage to erythrocytes, which results in methemoglobin and hemolytic anemia.[8] Both China and the World Health Organization have issued guidelines on chlorate and chlorite, each of which should be below 700 μg L^{-1} in drinking water.[9,10] Therefore, mitigating chlorate and chlorite pollution is imminent.

Many efforts have been made to control the pollution of halogenated DBPs,[11–16] including the use of adsorption, biological treatment and chemical oxidation methods. Deeudomwongsa *et al.*[12] removed DBP precursors by using ozonation and the peroxone process (H_2O_2/O_3). Ding *et al.* studied the adsorption performance of bromide by a magnetic ion exchange (MIEX) resin. Zhang *et al.*[16] used persulfate with 3D urchin-like CoO–CuO microparticles for DBP degradation. Among these methods, adsorption is widely used to remove DBPs in

School of Environment and Architecture, University of Shanghai for Science and Technology, Shanghai 200093, China. E-mail: fatzhxd@126.com; Fax: +86 021 55275979; Tel: +86 15921267160

† Electronic supplementary information (ESI) available. See DOI: 10.1039/c9ew01003c

Table 1 Experimental design conditions and response of each experimental run

Run	*A*: dosage (mL L^{-1})	*B*: reaction time (min)	*C*: initial concentration (mg L^{-1})	Actual value		Predicted value	
				Chlorate	Chlorite	Chlorate	Chlorite
1	6.00	30.00	2.25	85.56	72.5	85.56	72.50
2	6.00	30.00	2.25	85.56	72.5	85.56	72.50
3	2.00	30.00	0.50	72.19	53.49	73.19	56.57
4	2.00	0.00	2.25	0.00	0.00	−0.048	−2.30
5	10.00	30.00	0.50	74.94	73.92	75.17	72.02
6	10.00	0.00	2.25	0.00	0.00	0.72	2.68
7	6.00	30.00	2.25	85.56	72.50	85.56	72.50
8	6.00	0.00	4.00	0.00	0.00	0.28	0.40
9	6.00	30.00	2.25	85.56	72.50	85.56	72.50
10	10.00	60.00	2.25	82.72	80.38	81.27	82.68
11	6.00	60.00	4.00	85.02	71.89	85.97	72.67
12	10.00	30.00	4.00	82.27	79.00	82.77	75.92
13	6.00	30.00	2.25	85.56	72.50	85.56	72.50
14	2.00	60.00	2.25	80.29	59.46	79.57	56.78
15	6.00	0.00	0.50	0.00	0.00	−0.95	−0.78
16	2.00	30.00	4.00	79.52	58.57	79.29	60.47
17	6.00	60.00	0.50	75.3	66.43	75.02	66.03

Table 2 ANOVA test for response function *Y* (removal rate of chlorate and chlorite)

Source	Sum of squares	df	Mean square	*F*-Value	*p*-Value prob > *F*
Model	15 556.74	9	1728.53	229.38	<0.0001
A: dosage (mL L^{-1})	477.10	1	477.10	63.31	<0.0001
B: reaction time (min)	9671.62	1	9671.62	1283.43	<0.0001
C: initial concentration (mg L^{-1})	30.50	1	30.50	4.05	0.0841
AB	109.41	1	109.41	14.52	0.0066
AC	0.000	1	0.000	0.000	1.0000
BC	7.45	1	7.45	0.99	0.3531
A^2	36.33	1	36.33	4.82	0.0641
B^2	5041.40	1	5041.40	668.99	<0.0001
C^2	46.34	1	46.34	6.15	0.0422
Residual	52.75	7	7.54		
Lack of fit	52.75	3	17.58		
Pure error	0.000	4	0.000		
Cor total	15 609.49	16			

R^2 = 0.9966, adjusted R^2 = 0.9923, predicted R^2 = 0.9459.

water due to its low cost and simple set up and operation. Many materials have been applied to adsorb DBPs, such as Mg–Al hydrotalcite,[17] activated carbon,[18] MOFs[19] and MIEX.[14] However, these previous studies focused on bromate adsorption, with little investigation of the adsorption performances of the other two inorganic DBPs, chlorate and chlorite. MIEX resin has recently been developed as a promising technology for removing hazardous substances from raw water and wastewater.[20] MIEX resin, a strong basic anion resin, has a small particle size and large specific surface area, and exhibits fast adsorption compared with traditional resin.[21] In addition, MIEX has excellent regeneration performance in a saturated sodium chloride solution.[20] To the best of our knowledge, there are very few reports on the adsorption performance of chlorate and chlorite using MIEX. Similarly, the factors affecting the removal rate of chlorate and chlorite by MIEX, such as initial concentration, dosage of MIEX, bed volume, pH, coexistent anions, ion strength and organic matter, have not yet been researched systematically and completely.

Recently, response surface methodology (RSM) has been used to study the interaction between independent variables and dependent variables, to determine the optimal levels.[20] Lin *et al.*[22] optimized the method of cadmium removal by iron oxide nanoparticles using RSM. Fang *et al.*[23] optimized the method of phosphate removal by lanthanum oxide nanorods. Generally, RSM is an ideal solution for optimizing adsorption processes.

Hence, the purpose of this work was to evaluate the adsorption performance of chlorate and chlorite by MIEX. The adsorption behaviors of chlorate and chlorite and various factors (initial concentration, dosage of MIEX, bed volume, pH, coexistent anions, ion strength and organic matter) were investigated. The Box–Behnken design method was successfully used to optimize the operational conditions for removing chlorate and chlorite. In addition, a quadratic polynomial model was used to evaluate the effect of three key operating parameters: initial concentration, reaction time and dosage of adsorbent.

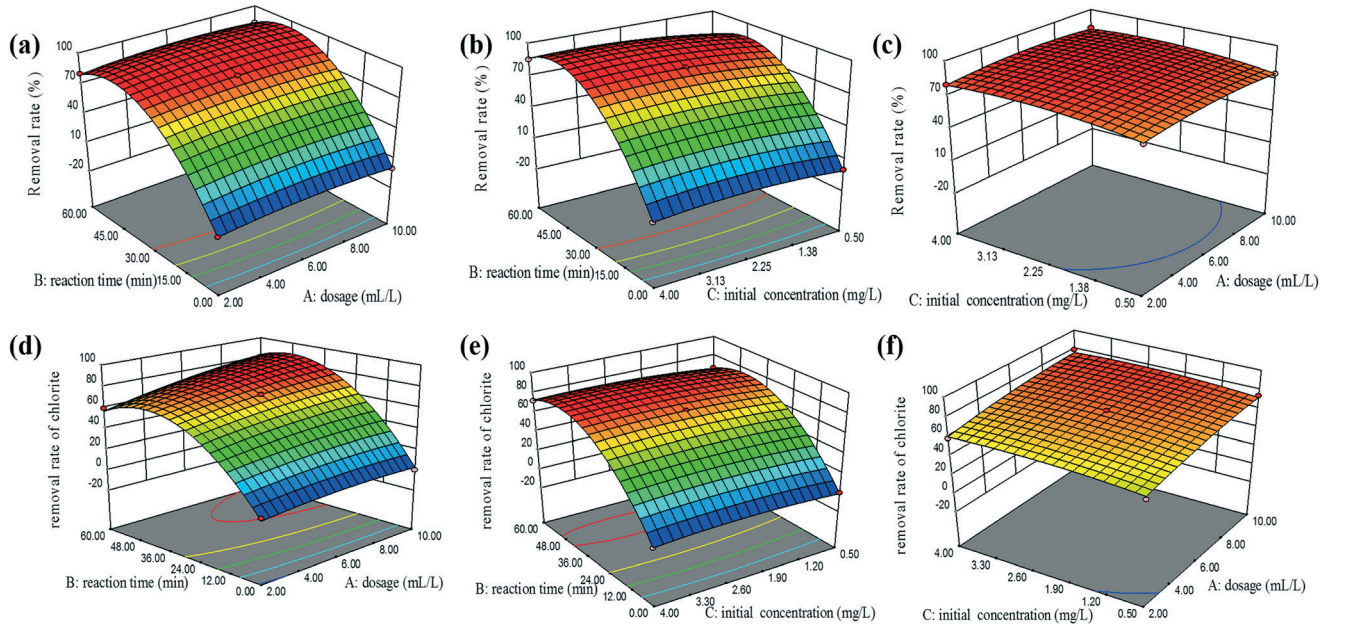

Fig. 1 3D plots of (a and d) the interactive effect of MIEX resin dosage and reaction time, (b and e) the interactive effect of bromate initial concentration and reaction time, and (c and f) the interactive effect of MIEX resin dosage and initial concentration, respectively.

2. Materials and methods

2.1. Materials

The MIEX resin was provided by Orica Watercare of Victoria. Chlorate ($NaClO_3$, 99%, Shanghai China) and chlorite ($NaClO_2$, 99%, Shanghai China) were used as the target pollutants. In this study, all the other reagents were purchased from Sinopharm Chemical Reagent Co., Ltd., China.

2.2. Characterization of MIEX resin

The morphology of MIEX resin beads was measured using scanning electron microscopy (SEM, VEGA3 TESCAN). Fourier transform infrared spectroscopy (FTIR, Nicolet/iS10) was used to test the functional groups.

2.3. Batch experiments

To research the adsorption behaviors of chlorate and chlorite on MIEX resin, batch experiments investigating the effect of pH (3–11), organic matter (1–8 mg L^{-1}), adsorbent dose (2–10 ml L^{-1}), ion strength (0.02–0.1 mmol L^{-1} as Na), coexistent anions (1 meq L^{-1}), initial solution pH (3–11), initial adsorbate (chlorate or chlorite) concentration (0.5–4 mg L^{-1}) and adsorption time (0–60 min) were implemented. MIEX resin (8 mL L^{-1}) was added to 1000 mL chlorate or chlorite solution (2 mg L^{-1}) and then the mixed solution was put into an agitator at room temperature for 60 min with a stirring rate of 250 rpm. 1 M NaOH and HCl solutions were used to adjust the initial pH value of the chlorate and chlorite solutions. Na_2SO_4, NaCl, Na_2CO_3 and $NaHCO_3$ were added into the chlorate and chlorite solutions to investigate the effect of coexistent anions.

2.4. Bed volume

10 mL MIEX resin was put into each of five beakers containing 1000 mL chlorate or chlorite solution (2 mg L^{-1}) at a stirring intensity of 250 rpm for 15 min. Then, 375, 187.5, 125, 94 and 75 ml samples of supernatant were placed into five new beakers (named 200, 400, 600, 800, 1000). Next, the remaining supernatant was removed and the 10 mL samples of MIEX resin were again placed into five beakers with 1000 mL chlorate or chlorite solution (2 mg L^{-1}) at the stirring intensity of 250 rpm for 15 min. This was repeated until the solution volume reached 750 mL, which meant that the MIEX resin had been used 2, 4, 6, 8, 10 times.

2.5. Isotherm adsorption

The adsorption experiments were performed using chlorate and chlorite (0.5–4 mg L^{-1}) interacting with 6 mL L^{-1} MIEX resin in centrifugal tubes. The experiments were conducted at 298 K for 60 min at a stirring intensity of 200 rpm in the shaker. After adsorption, the mixed solutions were centrifuged to obtain the supernatant, which was used to measure the concentration of chlorate and chlorite.

The adsorption amount of chlorate or chlorite onto the MIEX resin at equilibrium is calculated by the following equation:

$$q_e = \frac{(C_0 - C_e)\cdot V}{m} \quad (1)$$

where q_e (mg L^{-1}) is the amount of chlorite or chlorate adsorbed on the MIEX resin at equilibrium, C_0 (mg L^{-1}) is the initial concentration of chlorite or chlorate, C_e (mg L^{-1}) is the equilibrium concentration of chlorate or chlorite, V (L) is the volume of the mixed solutions, and m (L) is the volume of MIEX resin in this adsorption system.

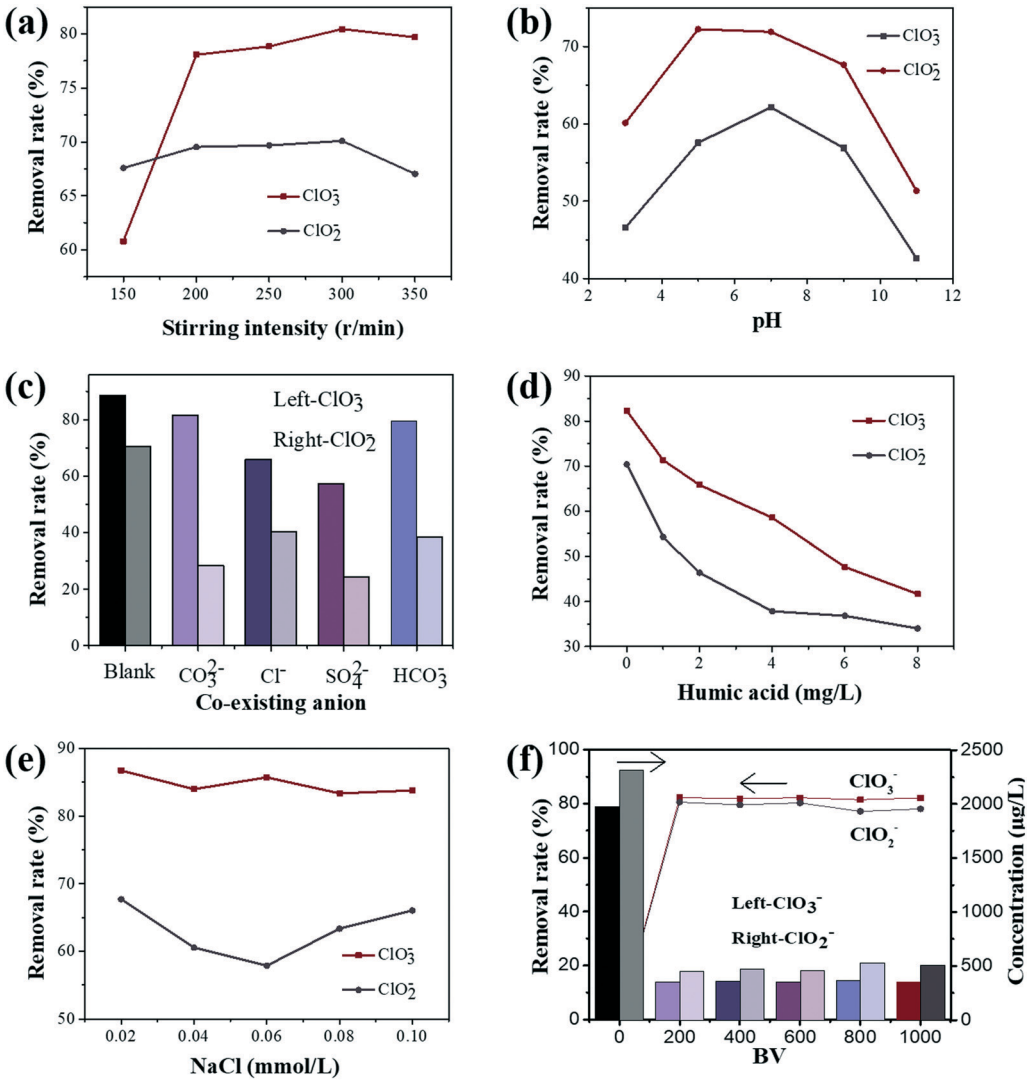

Fig. 2 (a) Effect of agitation intensity on bromate adsorption (conditions: 8.0 mL L^{-1} adsorbent, agitation speed 250 rpm). (b) Effect of initial pH on the adsorption of bromate onto MIEX resin (conditions: 8.0 mL L^{-1} adsorbent, agitation speed 250 rpm). (c) Effect of co-existing anions on the bromate adsorption (conditions: 8.0 mL L^{-1} adsorbent, agitation speed 250 rpm). (d) Effect of the natural organic matter (HA) on the bromate adsorption (conditions: 8.0 mL L^{-1} adsorbent, agitation speed 250 rpm). (e) Effect of ion strength on bromate adsorption (conditions: 8.0 mL L^{-1} adsorbent, agitation speed 250 rpm). (f) Effect of bed volume on bromate adsorption (conditions: 8.0 mL L^{-1} adsorbent, agitation speed 250 rpm).

The equilibrium data of isothermal adsorption were fitted to the Langmuir,[24] Freundlich[24] and Temkin[25] isotherm models. The Langmuir model is based on the assumption that the reaction process is monolayered and occurs at a specific uniform position on the adsorbent surface. The equation of the Langmuir model is the following:

$$q_e = \frac{q_m K_L C_e}{1 + K_L C_e} \quad (2)$$

where q_m (mg L^{-1}) is the adsorption capacity for chlorite or chlorate, and K_L (L mg^{-1}) is the constant of the Langmuir model.

The Freundlich model is an empirical equation, which assumes that the reaction process is multi-layered and occurs on a heterogeneous surface. The equation of the Freundlich model is the following:

$$q_e = K_F C_e^{\frac{1}{n}} \quad (3)$$

where K_F ($mg^{1-(1/n)}$ $L^{1/n}$ g^{-1}) is a constant of the Freundlich model, and $1/n$ is a constant of the reaction intensity of the Freundlich model.

The Tempkin model is also an empirical equation assumption. The equation of the Tempkin model is the following:

$$q_e = B \ln A + B \ln C_e \quad (4)$$

2.6. Kinetic adsorption

The chlorate and chlorite kinetic adsorption experiments start with the addition of 1000 ml chlorate or chlorite

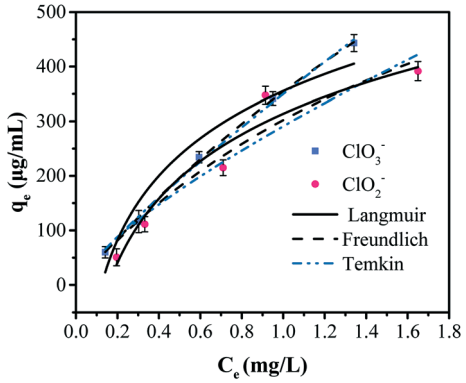

Fig. 3 Langmuir, Freundlich and Temkin isotherm for the adsorption of bromate onto MIEX resin (conditions: 1 L of adsorbate solution, adsorption time 60 min, agitation speed 250 rpm, temperature 298 K).

solution (0.5, 1, 2, 3, 4 mg L^{-1}) into 8 ml MIEX resin at a stirring intensity of 200 rpm and a temperature of 298 K. 5 ml of supernatant was taken in a syringe and filtrated through a 0.22 μm membrane filter at reaction times of 0, 1, 3, 5, 10, 20, 30, 45 and 60 min.

The intra-particle diffusion model, the pseudo-second-order (PSO) rate model and the pseudo-first-order (PFO)[26] rate model were used to fit the kinetic adsorption data. The three equations of these models are the following:

$$\frac{dq_t}{q_t} = k_1(q_e - q_t) \quad (5)$$

$$\frac{dq_t}{q_t} = k_2(q_e - q_t)^2 \quad (6)$$

$$q_t = k_i t^{0.5} + C \quad (7)$$

where q_t (mg mL^{-1}) is the amount of the chlorate or chlorite adsorbed at the time, k_1 (min^{-1}) is the constant of the PFO model, k_2 (mg mL^{-1} min^{-1}) is the constant of the PSO model; k_i is the diffusion rate constant (mg g^{-1} $h^{-0.5}$), and C (mg mL^{-1}) is the constant related to the thickness of the boundary layer. If the rate limiting step is intra-particle diffusion, the graph of q_t and the square root of time should be a straight line and pass through the origin (C = 0). The deviation between the graph and the linearity shows that the rate limiting step should be boundary layer (film) diffusion.

2.7. Response surface methodology

Design Expert software (version, 8.0.6) and Box–Behnken design (BBD) were used for designing and analyzing the response surface methodology experiments and results. The BBD approach with three levels (−1, 0, +1) can offer valid reports related to the interaction between three important parameters including the dosage of MIEX resin (A), the reaction time (B) and the initial concentration (C), which are given in Table S1.† According to the BBD, the 17 experiments are composed of the interaction of the three independent parameters, and the predicted responses to chlorate removal rate are given in Table 1. The following quadratic polynomial model expresses the mathematical relationship of the interaction of three independent parameters and the predicted responses:[27,28]

$$Y = \beta_0 + \sum_{i=1}^{k}\beta_i X_i + \sum_{i=1}^{k}\sum_{i=1}^{k}\beta_{ij} X_i X_j + \sum_{i=1}^{k}\beta_{ii} X_i^2 + \varepsilon \quad (8)$$

where Y is the value of the computational response, β_0 is the constant coefficient, β_i, β_{ii} and β_{ij} are the coefficients of the linear, quadratic and interactive terms individually for

Table 3 Isotherm parameters for chlorate and chlorite adsorption onto MIEX resin at 298 K

	Langmuir			Freundlich			Temkin		
Adsorbate	K_L	q_m	R^2	K_F	n	R^2	A	B	R^2
Chlorate	0.24	1792.1	0.998	349.9	1.16	0.996	169.7	8.11	0.947
Chlorite	0.48	931.6	0.929	290.9	1.34	0.903	169.9	6.33	0.947

Table 4 Kinetic parameters for chlorate and chlorite adsorption on MIEX resin

	Initial concentration	Pseudo-first-order kinetic model			Pseudo-second-order kinetic model		
Adsorbate	(mg L^{-1})	k_1	q_e	R^2	k_2	q_e	R^2
Chlorate	0.5	7.08	47.60	0.774	0.022	54.39	0.975
	1	66.07	116.47	0.797	0.009	133.00	0.994
	2	127.01	238.63	0.781	0.004	274.74	0.995
	3	3.34	288.19	0.484	0.001	380.56	0.943
	4	247.11	470.54	0.777	0.002	543.13	0.996
Chlorite	0.5	0.30	49.73	0.816	0.008	60.25	0.993
	1	1.56	100.62	0.659	0.006	121.09	0.984
	2	2.60	107.28	0.537	0.002	257.77	0.993
	3	19.50	296.10	0.504	0.002	368.77	0.984
	4	53.15	357.25	0.750	0.003	405.91	0.990

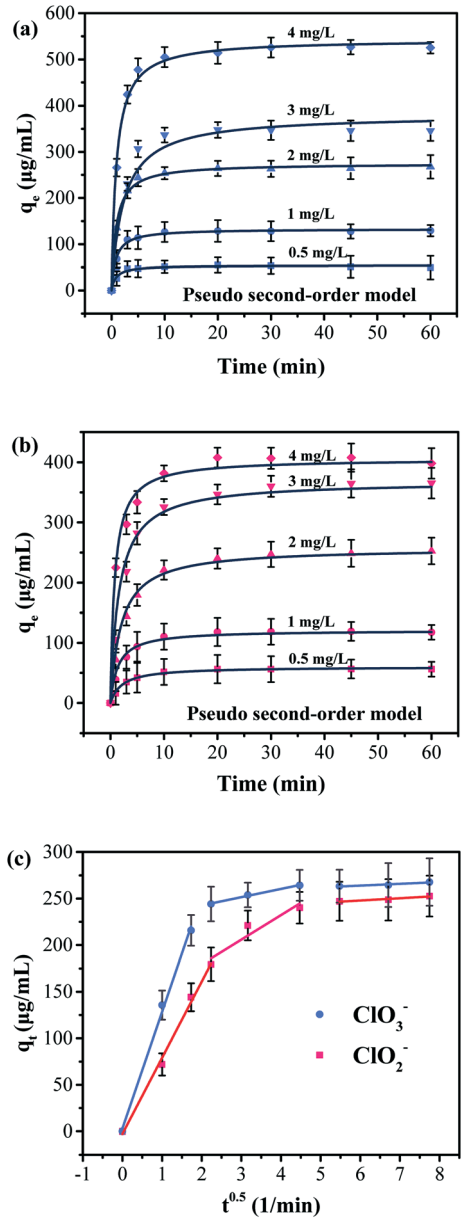

Fig. 4 The plots of pseudo-second-order model for (a) chlorate and (b) chlorite. (c) Intra-particle diffusion model for chlorate and chlorite adsorption on MIEX resin.

the parameter X_i, which have great effect on the predicted response. The correlation coefficient (R^2) is used to judge the match degree of the quadratic polynomial and the value of F is used for the statistical significance of the model.

2.8. Chlorate and chlorite detection

All the samples were handled using 0.22 μm polyether sulphone membranes. The chlorate and chlorite concentrations were detected using ion chromatography (Dionex ICS-2100, ThermoFisher, USA) with a suppressed conductivity detector. The effluent was 20 mM KOH and the current velocity was 1.0 mL min^{-1}. The injected volume of all the samples was 125 μL. The parathion column (Dionex IonPac AS19, 4.0 mm × 250 mm, ThermoFisher, USA) was operated at the temperature of 303 K.

3. Results and discussion

3.1. Analysis of RSM

3.1.1. BBD analysis. These chlorate and chlorite adsorption experiments were implemented according to the BBD model. The quadratic model equation predicts the relationship between the response (chlorate or chlorite removal rate) and three variables. The quadratic polynomial is as follows:

$$Y_1 = 85.56 + 0.99A + 40.42B + 3.05C + 0.61AB + 2.43BC - 3.83A^2 - 40.98B^2 - 4.50C^2 \quad (9)$$

$$Y_2 = 72.50 + 7.72A + 34.77B + 1.95C + 5.23AB + 1.36BC - 2.94A^2 - 34.60B^2 - 3.32C^2 \quad (10)$$

where Y_1 and Y_2 (%) are the removal rates of chlorate and chlorite, A (mL L^{-1}) is the code value for the dosage of MIEX resin, B is the code value for the reaction time, and C (mg L^{-1}) is the code value for the initial concentration.

3.1.2. ANOVA. The analysis of variance of the BBD analysis shown in Table 2 is significant ($P < 0.0001$) with two model F (3121.95 for chlorate and 229.38 for chlorite), indicating that the model is fit to describe the chlorate and chlorite adsorption onto MIEX.[29] Furthermore, the R^2 values of the regression equation are 0.9998 (chlorate) and 0.9966 (chlorite), respectively, indicating that the parameters (dosage, reaction time and initial concentration) explain 99.98% and 99.66% of the results of the experiments.[30] Therefore, the regression model can be used to predict the removal of chlorate and chlorite by MIEX. According to the model, the influence of the three parameters on the removal of chlorate and chlorite by MIEX follows the order: reaction time > the initial concentration > dosage (chlorate) and reaction time > dosage > the initial concentration (chlorite). The optimal removal conditions are dosage 6.67 mL L^{-1}, reaction time 45.26 min, initial concentration 3.08 mg L^{-1} for chlorate and dosage 9.62 mL

Table 5 The fitting parameters of intra-particle model

	Stage 1			Stage 2			Stage 3		
Adsorbate	k_1	C	R_2	k_2	C	R_2	k_3	C	R_2
Chlorate	125.2	3.1	0.993	8.9	224.88	0.986	0.2	252.43	0.907
Chlorite	78.82	2.5	0.993	26.3	126.77	0.815	2.4	233.19	0.921

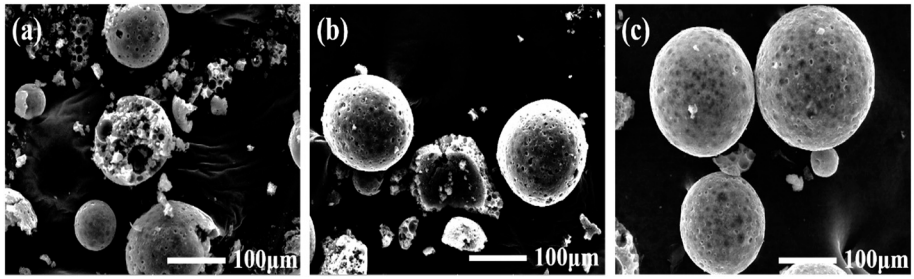

Fig. 5 SEM images of MIEX resin (a) before and (b and c) after adsorption.

L^{-1}, reaction time 46.36 min, initial concentration 3.04 mg L^{-1} for chlorite. The optimal removal rate of chlorate and chlorite are 96.65% and 89.41%, respectively.

3.1.3. Influence of interaction on the removal rate of chlorite and chlorate. 3D surface plots demonstrating the interaction relationship between the different factors affecting chlorate and chlorite removal rate are shown in Fig. 1. According to Fig. 1a and b, with the increase of the reaction time and dosage of MIEX, the removal rates of chlorate and chlorite increase. There are more adsorption active sites when the dosage of MIEX increases.[31,32] As shown in Fig. 1b and e, with the increase of the initial concentration, the removal rates increase. The results are consistent with the analysis of variance. However, the 3D surface plots (Fig. 1c and f) of the interaction between the initial concentration and dosage show a slower slope, indicating that their interaction is not significant, which is also consistent with the analysis of variance.

3.2. Effects of various factors for adsorption

3.2.1. Effect of stirring intensity. Fig. 2a exhibits the influence of the stirring intensity on the adsorption of chlorate and chlorite onto MIEX. With the increase of the rotation rate from 150 to 300 rpm, the amount of chlorate and chlorite adsorption increased from 60.8% to 80.4% and 67.5% to 70%, respectively. MIEX resin particles do not completely mix with chlorate and chlorite at a low stirring intensity such as 150 rpm. Therefore, chlorate and chlorite are not in full contact with the adsorption sites of the adsorbents, leading to a low removal rate. However, the amount of adsorption does not further increase when the stirring intensity is 350 rpm. This may be because the adsorption sites of MIEX resin are constant at specific concentration.

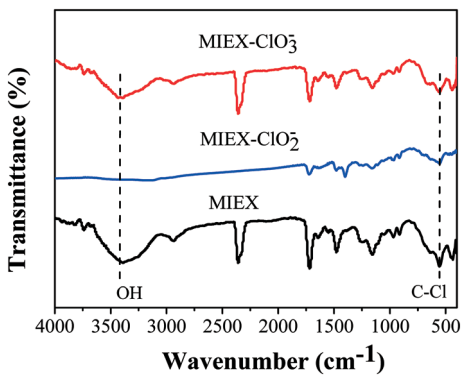

Fig. 6 FTIR spectra of MIEX before and after adsorbing chlorate and chlorite.

3.2.2. Effect of pH. pH is always an important factor in liquid phase removal. The results of the influence of different pH values on the adsorption of chlorate and chlorite by MIEX are shown in the Fig. 2b. With the increase in pH from 3 to 7, the removal rate of chlorate and chlorite increased from 60.1% to 71.9% and from 46.5% to 62.1%, respectively. This may be due to the presence of chloride ions in the solutions, resulting in competitive adsorption between chloride ions and chlorate or chlorite, when hydrochloric acid is used to regulate pH. However, when the pH was adjusted to alkaline, the amount of adsorption declined. This can also be explained by the competitive adsorption of hydroxyl with chlorate and chlorite. Ding *et al.*[14] investigated the adsorption behavior of bromate using MIEX resin and observed a similar result, due to the competitive adsorption of hydroxyl and bromine on MIEX resin.

3.2.3. Effect of anion coexistence. Inorganic anions, including chloride, sulfate and carbonate, are widely found in natural waters. Because of the different affinities between these inorganic anions and MIEX resin, the presence of inorganic anions may inhibit the adsorption of chlorate and chlorite. Therefore, investigating the effects of coexisting anions on the removal of chlorate and chlorite by MIEX resin is very important. The results of the effect of various anions on the removal of chlorate and chlorite are shown in Fig. 2c. The removal rates of chlorate and chlorite were found to be 88.7% and 70.3% with no other coexisting anions. However, in the presence of CO_3^{2-}, Cl^-, SO_4^{2-} and HCO_3^-, the removal rates of chlorate and chlorite declined. This indicates that each anion hinders the adsorption of chlorate and chlorite on MIEX to some extent. The effects of each anion on the adsorption of chlorate and chlorite by MIEX are different, and the sequence is as follows: $SO_4^{2-} > Cl^- > HCO_3^- > CO_3^{2-}$ (chlorate) and $SO_4^{2-} > CO_3^{2-} > HCO_3^- > Cl^-$ (chlorite). In addition, the effect may be compounded by the competitive adsorption between various different anions and chlorate or chlorite. Typically speaking, the higher valence anions have worse effects on the adsorbate adsorption onto the adsorbent. Cl^- and

HCO_3^- are usually easy to combine with the surface of MIEX to form an outer complex, which leads to ineffective competition. In a study by Li *et al.*,[33] the presence of SO_4^{2-} and PO_4^{3-} reduces the removal rate of vanadium more compared with Cl^-, NO_3^- and HCO_3^-. A similar result was observed for chlorite in the research. However, in this study, CO_3^{2-} has little effect on the adsorption of chlorate by MIEX. Tang *et al.*[34] studied the effect of the coexistence of anions on perchlorate removal, and found that PO_4^{3-} has little influence compared with SO_4^{2-}. This can be explained by the greater competitive capacity of chlorate compared with CO_3^{2-}.

3.2.4. Effect of organic matter. There is also a large amount of organic matter in natural waters, which influences the adsorption of some pollutants on MIEX.[34] In this investigation, the influence of the removal rates of chlorate and chlorite by MIEX using different concentrations of humic acid (HA) were analyzed, and the plot is exhibited in Fig. 2d. With the increase of HA from 0 to 8 mg L^{-1}, the removal rate of chlorate and chlorite decreased. This may be explained by the fact that the benzene ring of HA has a π–π interaction with the benzene ring of MIEX, resulting in the removal rate of chlorate and chlorite being decreased.[35] Jin *et al.* investigated the effect of HA on adsorption of PPCP by resin.[36] The intensity of the binding force between PPCP and HA can promote or inhibit adsorption. The binding forces between chlorate or chlorite and HA are too weak to promote their adsorption by MIEX. These mechanisms lead to the reduction of the adsorption capacity. However, when the concentration of HA was 4–8 mg L^{-1}, the reduction in the removal rate slowed down, because the number of active adsorption sites reaches a constant value beyond a certain concentration.

3.2.5. Effect of solution ionic strength. In this study, sodium chloride was used as the background electrolyte to investigate the factor of ionic strength on the adsorption of chlorate and chlorite. As shown in Fig. 2e, with the increase of the sodium chloride concentration from 0.02 mmol L^{-1} to 0.06 mmol L^{-1}, the adsorption amount of chlorate and chlorite by MIEX decreased. Competitive adsorption of Cl^- with chlorate and chlorite resulted in a decrease in the removal rate of chlorite and chlorate. The removal rate of chlorite increased gradually with an increase in the concentration of NaCl in increments of 0.1 mmol L^{-1}. This may be due to the strong repulsion between Cl^- adsorbed by MIEX resin and Cl^- in aqueous solution. Cl^- in solution is cannot easily bind to MIEX resin, while chlorite or chlorate occupies the adsorption sites on MIEX resin at this time. This makes the removal rate increase gradually.

3.2.6. Effect of bed volume. Bed volume is a key parameter in determining the regeneration cycle of MIEX resin. Fig. 2f shows the results of chlorate and chlorite adsorption by MIEX in various bed volumes. There is no significant difference in removal rate among various bed volumes. Theoretically, the smaller the bed volume, the greater the removal rates of chlorate and chlorite, but the removal rates of chlorate and chlorite are over 82.1% and 78.0%, respectively, for all bed volumes. Therefore, taking removal rate and cost into consideration, a larger bed volume should be selected for practical production.

3.3. Adsorption isotherms

The adsorption isotherms of chlorate and chlorite by MIEX are shown in Fig. 3. Due to the higher R^2 (Table 3), the Langmuir model fits better than the Freundlich and Temkin models. In addition, the adsorption of chlorate is higher than chlorite. MIEX resin is a kind of macroporous resin, which has the ability of magnetic ion exchange. When the temperature is low, the pores of the MIEX resin are narrowed, and it is difficult to produce new active adsorption sites.[37] At this point, the MIEX resin surface is almost smooth. In addition, the agglomeration process is inhibited at low temperature, so the process of chlorate and chlorite adsorption onto MIEX merely takes place at limited locations on the surface of MIEX. Generally speaking, the adsorption process of chlorate and chlorite onto MIEX can be better explained by the Langmuir model.

3.4. Adsorption kinetics

In this research, the adsorption kinetics of chlorate and chlorite at different initial concentrations of chlorate and chlorite (0.5–4 mg L^{-1}) is investigated. Simulation results of kinetics models of chlorate and chlorite adsorption by MIEX are given in Table 4, and the pseudo-second-order kinetic model fits better than chemical adsorption process because of the higher R^2. The plots of the pseudo-second-order kinetic model are exhibited in Fig. 4a and b. Chlorate and chlorite showed rapid adsorption in the first 10 min and then slower adsorption towards the equilibrium state. Therefore, the adsorption of chlorate and chlorite by MIEX resin consists of a chemical adsorption process involving valence forces through exchange or sharing of electrons between chlorate or chlorite ions and the adsorbent.[38] As shown in Table 4, with the increase of the initial concentration of chlorate and chlorite, the amount of adsorption increased from 54 to 525 μg mL^{-1} (chlorate) and from 60 to 398 μg mL^{-1} (chlorite). This may be due to the fact that increasing the initial chlorate or chlorite concentration increases the concentration gradient between the liquid and solid phases, resulting in an increase in the adsorption driving force.[39]

To further research the adsorption kinetic processes of chlorate and chlorite by MIEX resin, the intra-particle model is implemented, and the results are exhibited in Table 5 and Fig. 4c. The intra-particle diffusion curves show multiple linear relationships, indicating that the adsorption kinetics are controlled by a multistep mechanism. The adsorption process of adsorbent molecules or ions from the bulk liquid phase to porous solid adsorbents usually consists of three stages: film diffusion, intra-particle diffusion, and adsorptive attachment.[40] These steps are observed in chlorate and chlorite adsorption by MIEX resin, and the adsorption rate constants of the three steps decrease in the following sequence:

$k_1 > k_2 > k_3$, indicating that adsorption becomes gradually slower during the three steps. According to Table 5, the C values of stage 3 are bigger than those of stage 1 and 2, and the C values of chlorate are also bigger than those for chlorite. The C value reflects the thickness of the boundary layer. Increasing of the C value can reduce the change of internal mass transfer and increase the change in external mass diffusion.[41] Therefore, the adsorption process and film diffusion of chlorate and chlorite adsorption by MIEX can be controlled by intra-particle diffusion.

3.5. SEM and FTIR analysis

Fig. 5 exhibits the SEM plot of the MIEX resin before and after adsorption of chlorate and chlorite. As shown in Fig. 5a, the original resin beads are almost spherical, with a large number of pores and holes, which is conducive to the diffusion of chlorate and chlorite. In addition, the irregular and loose-layered structure on the surface of the MIEX resin particles greatly increases the specific surface area. The pattern of MIEX resin after adsorption is shown in Fig. 5b and c. For the MIEX resin particles, the pore size and hole size decreased obviously. The adsorbed resin is almost spherical with a smooth surface. This may be explained by the fact that the pores inside the resin are filled with chlorate and chlorite and the surface is also covered with chlorate and chlorite.

The FTIR plot is shown in Fig. 6. Generally, the adsorption peaks of MIEX resin after adsorption of chlorate and chlorite are weak, showing that some functional groups participate in the adsorption process. The adsorption peaks at 3413 cm^{-1} are assigned to O–H stretching[42,43] and become weakened after adsorption, owing to hydrogen bonding between MIEX and chlorate/chlorite. The peaks at 451 cm^{-1} are caused by asymmetric stretching and –C–O–C– symmetric stretching, proving the existence of polyacrylate structures. The peaks at 557 cm^{-1} are due to C–Cl vibrations, which weaken after chlorate and chlorite adsorption, indicating that the groups have joined the adsorption process. The mechanism is ion exchange through the displacement of Cl^- by nitrate ions.[44] The adsorption peaks at 1635 cm^{-1} and 1470 cm^{-1} are from the C=C stretching vibration of olefin and C=C skeleton vibration of benzene, individually, which represent the benzene ring and olefin structure of the MIEX resin. The stretching vibration peak of the hydrocarbon bond arises at 2939 cm^{-1}. In addition, after the MIEX resin adsorbs chlorate and chlorite, the adsorption peaks of the functional groups show certain deviations, as shown in Fig. 6, suggesting that the adsorption process is controlled by both chemical adsorption and physical adsorption.

Conclusions

The results of this study show that MIEX resin can be used as an effective adsorbent for chlorate and chlorite. When the adsorbent dosage is increased, the removal rates of chlorate and chlorite increase. For chlorate and chlorite adsorption onto MIEX resin, 250 rpm is an optimal stirring strength. When the pH is neutral, the highest removal efficiency of chlorate and chlorite by MIEX can be achieved. Coexistent anions have great effect on chlorate and chlorite removal and the sequence is given as follows: $SO_4^{2-} > Cl^- > HCO_3^- > CO_3^{2-}$ (chlorate) and $SO_4^{2-} > CO_3^{2-} > HCO_3^- > Cl^-$ (chlorite). The Langmuir model fits the adsorption isotherm well. Furthermore, the kinetics process of chlorate and chlorite was well represented by a pseudo-second-order model. The pseudo-second-order model was successfully applied to describe the kinetics adsorption of chlorate and chlorite by MIEX. The Box–Behnken design method was successfully used to establish a quadratic polynomial mode for predicting the removal efficiency of chlorate and chlorite, which is composed of three variables (adsorbent dosage, reaction time and initial concentration). According to the results, the adsorbent dosage had a strong interaction with the chlorate or chlorite concentration and reaction time, which has a significant impact on the optimization of the chlorate and chlorite removal process by MIEX.

Conflicts of interest

There are no conflicts to declare.

Acknowledgements

The study was funded by the National Natural Science Foundation of China (No. 51508327). The fund focuses on the removal of contaminants from water.

References

1 C. Zhang, H. Huang, G. Li, L. Wang, L. Song and X. Li, Zeolitic acidity as a promoter for the catalytic oxidation of toluene over MnOx/HZSM-5 catalysts, *Catal. Today*, 2019, **327**, 374–381.
2 Z. Wang, Q. Sun, D. Wang, Z. Hong, Z. P. Qu and X. B. Li, Hollow ZSM-5 zeolite encapsulated Ag nanoparticles for SO_2 resistant selective catalytic oxidation of ammonia to nitrogen, *Sep. Purif. Technol.*, 2019, **209**, 1016–1026.
3 L. Wang, G. Y. Yin, Y. Q. Yang and X. D. Zhang, Enhanced CO oxidation and toluene oxidation on CuCeZr catalysts derived from UiO-66 metal organic frameworks, *React. Kinet., Mech. Catal.*, 2019, **128**, 193–204.
4 C. H. Zhang, K. Zeng, C. Wang, X. H. Liu, G. L. Wu, Z. Wang and D. Wang, $LaMnO_3$ perovskites via a facile nickel substitution strategy for boosting propane combustion performance, *Ceram. Int.*, 2020, DOI: 10.1016/j.ceramint.2019.11.153.
5 M. D. Zhou, Z. Wang, Q. Sun, J. Y. Wang, C. H. Zhang, D. Chen and X. B. Li, High Performance Ag-Cu Nanoalloy Catalyst for the Selective Catalytic Oxidation of Ammonia, *ACS Appl. Mater. Interfaces*, 2019, **11**, 46875–46885.
6 W. Gan, S. Huang, Y. Ge, T. Bong, P. Westerhoff, J. Zhai and X. Yang, Chlorite formation during ClO_2 oxidation of model compounds having various functional groups and humic substances, *Water Res.*, 2019, **159**, 348–357.

7 F. Al-Otoum, M. A. Al-Ghouti, T. A. Ahmed and M. Abu-Dieyeh, Disinfection by-products of chlorine dioxide (chlorite, chlorate, and trihalomethanes): Occurrence in drinking water in Qatar, *Chemosphere*, 2016, **164**, 649–656.
8 E. M. Aieta and J. D. Berg, A review of chlorine dioxide in drinking water treatment, *J. - Am. Water Works Assoc.*, 1986, **78**, 62–72.
9 E. X. Li, C. J. Chen and L. Zhang, Study on standard for drinking water quality in China, *Aibian, Jibian, Tubian*, 2007, **19**, 168–170.
10 F. Edition, Guidelines for drinking-water quality, *WHO Chron.*, 2011, **38**, 104–108.
11 J. Fu, W. N. Lee, C. Coleman, K. Nowack, J. Carter and C. H. Huang, Removal of disinfection byproduct (DBP) precursors in water by two-stage biofiltration treatment, *Water Res.*, 2017, **123**, 224–235.
12 P. Deeudomwongsa, S. Phattarapattamawong and K. Y. A. Lin, Control of disinfection byproducts (DBPs) by ozonation and peroxone process: role of chloride on removal of DBP precursors, *Chemosphere*, 2017, **184**, 1215–1222.
13 D. Metcalfe, C. Rockey, B. Jefferson, S. Judd and P. Jarvis, Removal of disinfection by-product precursors by coagulation and an innovative suspended ion exchange process, *Water Res.*, 2015, **87**, 20–28.
14 L. Ding, H. Deng, C. Wu and X. Han, Affecting factors, equilibrium, kinetics and thermodynamics of bromide removal from aqueous solutions by MIEX resin, *Chem. Eng. J.*, 2012, **181**, 360–370.
15 D. M. Drennan, R. E. Koshy, D. B. Gent and C. E. Schaefer, Electrochemical treatment for greywater reuse: effects of cell configuration on COD reduction and disinfection byproduct formation and removal, *Water Supply*, 2019, **19**, 891–898.
16 X. Zhang, Q. Lin, H. Luo, R. Huang, R. Xiao and Q. Liu, Activation of persulfate with 3D urchin-like CoO-CuO microparticles for DBP degradation: A catalytic mechanism study, *Sci. Total Environ.*, 2019, **655**, 614–621.
17 H. Ji, W. Wu, F. Li, X. Yu, J. Fu and L. Jia, Enhanced adsorption of bromate from aqueous solutions on ordered mesoporous Mg-Al layered double hydroxides (LDHs), *J. Hazard. Mater.*, 2017, **334**, 212–222.
18 S. Hong, S. Deng, X. Yao, B. Wang, Y. Wang, J. Huang and G. Yu, Bromate removal from water by polypyrrole tailored activated carbon, *J. Colloid Interface Sci.*, 2016, **467**, 10–16.
19 P. Han and Y. Xia, Thiol-functionalized metal-organic framework for highly efficient removal of bromate from water, *J. Environ. Chem. Eng.*, 2018, **6**, 3384–3391.
20 Y. Yang, Q. Ding, M. Yang, Y. Wang, N. Liu and X. Zhang, Magnetic ion exchange resin for effective removal of perfluorooctanoate from water: study of a response surface methodology and adsorption performances, *Environ. Sci. Pollut. Res.*, 2018, **25**, 29267–29278.
21 X. Lu, Y. Shao, N. Gao and L. Ding, Equilibrium, thermodynamic, and kinetic studies of the adsorption of 2, 4-dichlorophenoxyacetic acid from aqueous solution by MIEX resin, *J. Chem. Eng. Data*, 2015, **60**, 1259–1269.
22 J. Lin, B. Su, M. Sun, B. Chen and Z. Chen, Biosynthesized iron oxide nanoparticles used for optimized removal of cadmium with response surface methodology, *Sci. Total Environ.*, 2018, **627**, 314–321.
23 L. Fang, B. Wu, J. K. Chan and I. M. Lo, Lanthanum oxide nanorods for enhanced phosphate removal from sewage: a response surface methodology study, *Chemosphere*, 2018, **192**, 209–216.
24 J. Luo, M. Sun, C. Ritt, X. Liu, Y. Pei, J. C. Crittenden and M. Elimelech, Tuning Pb (II) Adsorption from Aqueous Solutions on Ultrathin Iron Oxychloride (FeOCl) Nanosheets, *Environ. Sci. Technol.*, 2019, **53**, 2075–2085.
25 Z. U. Ahmad, L. Yao, J. Wang, D. D. Gang, F. Islam and M. E. Zappi, Neodymium embedded ordered mesoporous carbon (OMC) for enhanced adsorption of sunset yellow: Characterizations, adsorption study and adsorption mechanism, *Chem. Eng. J.*, 2019, **359**, 814–826.
26 G. Z. Kyzas, G. Bomis, R. I. Kosheleva, E. K. Efthimiadou, E. P. Favvas, M. Kostoglou and A. C. Mitropoulos, Nanobubbles effect on heavy metal ions adsorption by activated carbon, *Chem. Eng. J.*, 2019, **356**, 91–97.
27 B. D. Yirsaw, M. Megharaj, Z. Chen and R. Naidu, Reduction of hexavalent chromium by green synthesized nano zero valent iron and process optimization using response surface methodology, *Environ. Technol. Inno.*, 2016, **5**, 136–147.
28 M. Savasari, M. Emadi, M. A. Bahmanyar and P. Biparva, Optimization of Cd (II) removal from aqueous solution by ascorbic acid-stabilized zero valent iron nanoparticles using response surface methodology, *J. Ind. Eng. Chem.*, 2015, **21**, 1403–1409.
29 M. A. Watson, A. Tubić, J. Agbaba, J. Nikić, S. Maletić, J. M. Jazić and B. Dalmacija, Response surface methodology investigation into the interactions between arsenic and humic acid in water during the coagulation process, *J. Hazard. Mater.*, 2016, **312**, 150–158.
30 G. I. Danmaliki, T. A. Saleh and A. A. Shamsuddeen, Response surface methodology optimization of adsorptive desulfurization on nickel/activated carbon, *Chem. Eng. J.*, 2017, **313**, 993–1003.
31 Q. Peng, M. Liu, J. Zheng and C. Zhou, Adsorption of dyes in aqueous solutions by chitosan–halloysite nanotubes composite hydrogel beads, *Microporous Mesoporous Mater.*, 2015, **201**, 190–201.
32 W. Liu, X. Zhao, T. Wang, D. Zhao and J. Ni, Adsorption of U (VI) by multilayer titanate nanotubes: effects of inorganic cations, carbonate and natural organic matter, *Chem. Eng. J.*, 2016, **286**, 427–435.
33 M. Li, B. Zhang, S. Zou, Q. Liu and M. Yang, Highly Selective Adsorption of Vanadium (V) by Nano-Hydrous Zirconium Oxide-Modified Anion Exchange Resin, *J. Hazard. Mater.*, 2019, 121386.
34 Y. Tang, S. Liang, H. Guo, H. You, N. Gao and S. Yu, Adsorptive characteristics of perchlorate from aqueous solutions by MIEX resin, *Colloids Surf., A*, 2013, **417**, 26–31.
35 F. F. Liu, J. Zhao, S. Wang and B. Xing, Adsorption of sulfonamides on reduced graphene oxides as affected by pH

and dissolved organic matter, *Environ. Pollut.*, 2016, **210**, 85–93.

36 J. Jin, T. Feng, R. Gao, Y. Ma, W. Wang, Q. Zhou and A. Li, Ultrahigh selective adsorption of zwitterionic PPCPs both in the absence and presence of humic acid: Performance and mechanism, *J. Hazard. Mater.*, 2018, **348**, 117–124.

37 L. Ding, X. Lu, H. Deng and X. Zhang, Adsorptive removal of 2, 4-dichlorophenoxyacetic acid (2, 4-D) from aqueous solutions using MIEX resin, *Ind. Eng. Chem. Res.*, 2012, **51**, 11226–11235.

38 M. Al-Ghouti, M. A. M. Khraisheh, M. N. M. Ahmad and S. Allen, Thermodynamic behaviour and the effect of temperature on the removal of dyes from aqueous solution using modified diatomite: a kinetic study, *J. Colloid Interface Sci.*, 2005, **287**, 6–13.

39 B. Noroozi, G. A. Sorial, H. Bahrami and M. Arami, Equilibrium and kinetic adsorption study of a cationic dye by a natural adsorbent—Silkworm pupa, *J. Hazard. Mater.*, 2007, **13**, 167–174.

40 J. Wang, Z. Li, N. Hu, L. Liu, C. Huang, Q. Yang and J. Wang, From lamellar to hierarchical: overcoming the diffusion barriers of sulfide-intercalated layered double hydroxides for highly efficient water treatment, *J. Hazard. Mater.*, 2017, **5**, 22506–22511.

41 W. Sun, H. Li, H. Li, S. Li and X. Cao, Adsorption mechanisms of ibuprofen and naproxen to UiO-66 and UiO-66-NH2: Batch experiment and DFT calculation, *Chem. Eng. J.*, 2019, **360**, 645–653.

42 R. Hans, G. Senanayake, L. C. S. Dharmasiri, J. A. P. Mathes and D. J. Kim, A preliminary batch study of sorption kinetics of Cr (VI) ions from aqueous solutions by a magnetic ion exchange (MIEX®) resin and determination of film/pore diffusivity, *Hydrometallurgy*, 2016, **164**, 208–218.

43 Y. Wang, L. Yu, R. T. Wang, Y. Wang and X. D. Zhang, Microwave catalytic activities of supported perovskite catalysts MOx/LaCo0.5Cu0.5O3@CM (M = Mg, Al) for salicylic acid degradation, *J. Colloid Interface Sci.*, 2019, **564**, 392–405.

44 Z. Ren, X. Xu, X. Wang, B. Gao, Q. Yue, W. Song and H. Wang, FTIR, Raman, and XPS analysis during phosphate, nitrate and Cr (VI) removal by amine cross-linking biosorbent, *J. Colloid Interface Sci.*, 2016, **468**, 313–323.

